Check for updates

plant biology

Plant Biology ISSN 1435-8603

RESEARCH ARTICLE

Overview of transcriptome changes and phenomic profile of sanitized artichoke vis-à-vis non-sanitized plants

R. Spanò[1], A. Petrozza[2], S. Summerer[2], S. Fortunato[3], M. C. de Pinto[3], F. Cellini[2] & T. Mascia[1]

1 Department of Soil, Plant and Food Sciences, University of Bari "Aldo Moro", Bari, Italy
2 Agenzia Lucana di Sviluppo e di Innovazione in Agricoltura (ALSIA), Centro Ricerche Metapontum Agrobios, Metaponto di Bernalda, Italy
3 Department of Bioscience, Biotechnology and Environment, University of Bari "Aldo Moro", Bari, Italy

Keywords
lignin; peroxidase; plant phenotyping; RNAseq analysis; sanitation protocol; virus infection.

Correspondence
R. Spanò, Department of Soil, Plant and Food Sciences, University of Bari "Aldo Moro", Via Amendola 165/A, Bari 70126, Italy.
E-mail: roberta.spano@uniba.it;

Editor
V. Pastor

Received: 27 March 2024;
Accepted: 19 May 2024

doi:10.1111/plb.13675

ABSTRACT

- Plant tissue *in vitro* culture is increasingly used in agriculture to improve crop production, nutritional quality, and commercial value. In plant virology, the technique is used as sanitation protocol to produce virus-free plants. Sanitized (S) artichokes show increased vigour compared to their non-sanitized (NS) counterparts, because viral infections lead to a decline of growth and development.
- To investigate mechanisms that control the complex traits related to morphology, growth, and yield in S artichokes compared to NS plants, RNAseq analysis and phenotyping by imaging were used. The role of peroxidases (POD) was also investigated to understand their involvement in sanitized plant development.
- Results showed that virus infection affected regulation of cell cycle, gene expression and signal transduction modulating cellular response to stimulus/stress. Moreover, primary metabolism and photosynthesis were also influenced, contributing to explain the main morphological differences observed between S and NS artichokes. Sanitized artichokes are also characterized by higher POD activity, probably associated with increased plant growth, rather than strengthening of cell walls.
- Overall, results show that the differences in development of S artichokes may be derived from the *in vitro* culture stressor, as well as through pathogen elimination, which, in turn, improve qualitative and quantitative artichoke production.

INTRODUCTION

Virus infection can significantly damage globe artichoke (*Cynara cardunculus* L. subsp. *scolymus*) crops, reducing yield and quality. In the Mediterranean Basin, the most common plant viruses affecting artichoke are RNA viruses, namely artichoke latent virus (ArLV), artichoke Italian latent virus (AILV), artichoke mottled crinkle virus (AMCV), cucumber mosaic virus (CMV), tomato infectious chlorosis virus (TICV) and tomato spotted wilt virus (TSWV) (Spanò *et al.* 2018). In general, symptoms of viral diseases in globe artichoke may include yellowing, malformation and distortion of leaves and flowers, delayed flowering, or no inflorescence development. In addition, viral infections can increase susceptibility to other common pathogens, such as *Verticillium dahliae*, affecting normal development of the plant (Cirulli *et al.* 2010), or the crown rot agents *Sclerotinia sclerotiorum*, *Sclerotium rolfsii* (Aydoğdu *et al.* 2016) and *Rhizoctonia solani*. Also economically relevant are infections caused by *Leveillula taurica* f.sp. *cynarae* and *Bremia lactucae* on leaves, and *Botrytis cinerea*, specially on immature inflorescences (capitula) (Corda *et al.* 1982). Several other bacterial diseases and pests can significantly damage production (Penalver *et al.* 1994), further complicating the symptomatology of virus-infected artichoke plants.

The occurrence of infectious artichoke viruses in the Mediterranean Basin is a major concern for farmers because of the yield-limiting potential of these pathogens. Crop rotation and preventing insect vector spread are common management strategies that are adopted to avoid virus infection and transmission through vegetative propagation, in addition to the use of virus-free certified plant material (Spanò *et al.* 2018).

The production of certified virus-free artichoke can be based on *in vitro* meristem tip culture combined with a thermotherapy treatment (Spanò *et al.* 2018). This sanitation protocol can ensure higher productivity, quality and vigour and reduce the need for chemical treatments and fertilizers, thus promoting sustainable agricultural practices. It can also prevent phytosanitary risks, avoid genetic erosion and consequent loss of germplasm resources.

Apulia (southern Italy) hosts many artichoke ecotypes, principally divided between early flowering types (producing capitula between autumn and spring) and late flowering types (producing capitula during spring and early summer), which have recently undergone a sanitation programme and *ex situ* conservation (Spanò *et al.* 2018). However, sanitation protocols, against biotic and abiotic stresses, may induce important transcriptome changes (Spanò *et al.* 2023). To investigate the regulatory mechanisms that control gene expression after sanitation treatments, this study used transcriptome and phenotyping analyses to unravel complex biological processes related to the metabolic pathways, development and stress responses in sanitized (S) artichoke compared to non-sanitized (NS) plants of the Apulian early flowering ecotype Brindisino.

Plant Biology © 2024 The Author(s). *Plant Biology* published by John Wiley & Sons Ltd on behalf of German Society for Plant Sciences, Royal Botanical Society of the Netherlands.
This is an open access article under the terms of the Creative Commons Attribution License, which permits use, distribution and reproduction in any medium, provided the original work is properly cited.

Class III peroxidase (POD) activity and lignin accumulation, in addition to transcriptomic and plant phenotype profiles, contribute to understanding the mechanisms involved in better development and vigour observed in S compared to NS plants. This unique study combines phenotype parameters and molecular traits after *in vitro* meristem tip culture and thermotherapy, evidencing molecular, biochemical, and physiological markers through which S plants are distinguished from virus-infected NS plants.

MATERIAL AND METHODS

Plant material and total rna extraction

Agronomic and qualitative traits of 1-year-old sanitized (S) and non-sanitized (NS) early-flowering Brindisino ecotypes grown in a comparative field in Brindisi province (Apulia, southern Italy), were preliminary evaluated using the International Union for the Protection of new Varieties of Plants descriptors (https://www.upov.int/test_guidelines/en/list.jsp, accessed on January 2023) in late December 2020. Total number of flower heads produced, height and average plant diameter, main stem diameter, leaf length (Cravero *et al.* 2007) and market demand fot each ecotype are the main features used for agronomic comparative analysis between S and NS Brindisino ecotypes.

Differences between S and NS Brindisino ecotypes were also analysed at molecular, biochemical and phenotypic levels using plant material collected in late September 2021, before production begins. To avoid biases introduced by the operator, a systematic random sampling design (Barnett 1986) was used to select young artichoke offshoots (10–15 cm in length) of ten NS stocks, from a commercial open-field crop located in Brindisi province, and of ten sanitized stock, from a primary source germplasm greenhouse equipped with anti-aphid nets, to prevent re-infection (Spanò *et al.* 2018), in a commercial nursery (Vivaio F.lli Corrado, Torre Santa Susanna, Brindisi, Apulia, Italy). To reduce biases introduced by the different origins, all collected offshoots were transplanted into 18-cm diameter pots (3.5 L) containing a substrate of brown and white peat (1:4, v:v), mixed with expanded clay. Plants were maintained *ex situ* in a greenhouse at 18–20 °C, 55–60% relative humidity (RH) and 16 h light/8 h dark photoperiod until used for further experiments. Plants developed from such offshoots were considered biological replicates of the non-sanitized and sanitized phytosanitary condition and were hereafter denoted NS and S plants.

Total RNA was obtained from 100 mg fresh leaf material of S and NS plants (in triplicate) ground in liquid nitrogen and extracted following the EuroGOLD RNAPure™ (EuroClone, Pero, Italy) protocol. RNA concentration and quality were estimated with the Qubit RNA HS assay kit (ThermoFisher Scientific, Waltham, MA, USA), agarose gel electrophoresis and Bioanalyzer, RNA 6000 Pico Labchip (Agilent Technologies, Santa Clara, CA, USA). Samples with RNA integrity number (RIN) ≥ 7 were used for evaluation of phytosanitary status and results from RNA sequencing experiments.

Virus hybridization assay

The presence of the most relevant viruses in samples collected from NS and S plants was assessed by digoxigenin-labelled polyprobe hybridization, as described by Minutillo *et al.* (2021). This assay allows simultaneous detection of artichoke Italian latent virus (AILV), artichoke latent virus (ArLV), artichoke mottled crinkle virus (AMCV), turnip mosaic virus (TuMV), tomato infectious chlorosis virus (TICV), bean yellow mosaic virus (BYMV), cucumber mosaic virus (CMV), pelargonium zonate spot virus (PZSV), tomato spotted wilt virus (TSWV) and tobacco mosaic virus (TMV). Nylon membranes were spotted with 500 ng total RNA extracted as previously described from S and NS fresh tissue.

RNA sequencing and transcriptome analysis

The RNA extracted from samples of NS and S plants was ribo-depleted and reverse transcribed to prepare complementary DNA (cDNA) libraries. An Illumina HiSeq 2×150 bp reads platform (GENEWIZ, Azenta Life Sciences, Leipzig, Germany) were used to obtain sequencing data. Raw reads were analysed using the Galaxy platform (https://usegalaxy.eu, accessed April 2023) tools as described by Spanò *et al.* (2023). Reads were mapped on *C. cardunculus* genome sequence (Acc. GCA_001531365.1) and used to validate virus detection and for gene expression analysis.

Unmapped reads on the *C. cardunculus* genome were aligned against AILV (GeneBank Acc. LT608395.1 and LT608396.1 for RNA1 and RNA2, respectively), ArLV (GeneBank Acc. KF155694.1), AMCV (GeneBank Acc. NC_001339.1), TuMV (GeneBank Acc. AP017717.1), TICV (GeneBank Acc. NC_013258.1 and NC_013259.1 for RNA1 and RNA2, respectively), BYMV (GeneBank Acc. HG970854.1), CMV (GeneBank Acc. NC_002034.1, NC_002035.1 and NC_001440.1 for RNA1, RNA2 and RNA3, respectively), PZSV (GeneBank Acc. AJ272327.1, AJ272328.2 and AJ272329.1 for RNA1, RNA2 and RNA3, respectively), TSWV (GeneBank Acc. KT717691.1, KT717692.1 and KT717693.1 for RNA1, RNA2 and RNA3, respectively) and TMV (GeneBank Acc. AB369276.1) genome sequences by running the Bowtie2 tool (Langmead *et al.* 2009; Langmead & Salzberg 2012). Read alignment was visualized using Integrative Genomics Viewer (IGV) (Robinson *et al.* 2011; Thorvaldsdóttir *et al.* 2013). Reads mapped on a specific virus genome were validated by polymerase chain reactions (PCR) according to Minutillo *et al.* (2012).

Differentially expressed genes (DEGs) between S and NS sample conditions were calculated using the DESeq2 tool (Love *et al.* 2014) with default parameters. In detail, the logarithm (basis 2) of the fold change of S *vs* NS conditions tested ≥ 1 or ≤ -1 ($|\log_2 FC| \geq 1$) were considered significantly differentially expressed with a false discovery rate (FDR) ≤ 0.05 (Benjamini & Hochberg 1995; Spanò *et al.* 2023). The resulting DEGs were used for gene ontology functional enrichment analysis using the g:GOSt tool on the g:Prifiler2 web server (https://biit.cs.ut.ee/gprofiler/gost, version *e109_eg56_p17*_1d3191d, accessed June 2023) and divided in three Gene Ontology (GO) main category: molecular function (MF), biological process (BP) and cellular component (CC). The BlastKOALA tool (https://www.kegg.jp/blastkoala/, accessed June 2023) was used for a detailed functional characterization of upregulated and downregulated DEGs (Kanehisa *et al.* 2016) based on KEGG database resource (https://www.kegg.jp/, accessed June 2023).

14388677, 0, Downloaded from https://onlinelibrary.wiley.com/doi/10.1111/plb.13675 by CNR Group, Wiley Online Library on [11/07/2024]. See the Terms and Conditions (https://onlinelibrary.wiley.com/terms-and-conditions) on Wiley Online Library for rules of use; OA articles are governed by the applicable Creative Commons License

Phenotyping platform and data acquisition process

Six plants obtained from for each S and NS condition were transferred to the ALSIA (Agenzia Lucana di Sviluppo ed Innovazione in Agricoltura, Metaponto, MT) (Genangeli *et al.* 2023) laboratory and grown in a non-conditioned greenhouse. Temperature and RH were monitored throughout the experiment and plants were automatically irrigated with emergency irrigation. The phenotyping experiment was performed using a LemnaTec Scanalzer 3D system for the high-throughput plant phenotyping (HTPP) analysis. A balance installed on the pot conveyor belt of the HTPP platform measured loss-in-weight of each pot to calculate watering volumes. The phenotyping status of S and NS plants was measured from April to May 2022. Four sequential cameras installed in the HTPP platform took phenotyping 3D images of plants. Images acquired per plant were: two sideview in the near-infrared (NIR) and three in the visible light (RGB). The plants were illuminated by halogen lamps with a maximum level variation of 2% and net power of 35 W. Spectral acquisitions were carried out simultaneously with RGB acquisitions. Collected images were subjected to a segmentation process and retrievals were performed using Python 3.8 with the PlantCV package v3.9 (https://plantcv.danforthcenter.org/). Pixel values of each image were computed to obtain the following optical indices (OIs): projected shoot area (PSA); height above reference; solidity; NIR; Senescence Index (SI); and HUE Index (HUE).

Projected shoot area (PSA) is the sum of the number of pixels inside the plant region in each of the three orthogonal RGB images, computed as follows (Golzarian *et al.* 2011):

$$\mathrm{PSA} = \mathrm{TA(x)} + \mathrm{TA(y)} + \mathrm{TA(z)} \quad (1)$$

where TA(x) is the target top area, TA(y) is the target side area and TA(z) is the target side area rotated 90°; the result is the sum of all three areas expressed in cm^2.

Height above reference is the pixel height of the plant calculated from colour images and converted in cm. Height above reference was measured from the top of the pot as reference point divided by the base of a single plant.

Solidity is the ratio of area of the plant projection divided by the area of a convex hull containing the plant projection. This value is calculated from one top view image of a single plant.

Near infrared (NIR) is the physical association between leaf properties and light reflectance based on structure and chemical composition of leaves at 700–1100 nm wavelengths. This value measures the photon penetration distance, which is particularly useful to investigate leaf composition, function and diversity.

Senescence Index (SI) is an optical index expressed as a percentage used to define senescence status in plants, computed following Sancho-Adamson *et al.* (2019):

$$\mathrm{SI} = \frac{(\mathrm{GAS} - \mathrm{GerAS})}{\mathrm{GAS}} \quad (2)$$

where GAS is green area in a side view, and the corresponding value is the sum of pixel values in the HUE index angular region from 60° to 180°. GerAS is a greener area in the side view obtained from the sum of pixel values in the HUE angular region from 80° to 180°.

The HUE index is a single number corresponding to an angular position, from 0° to 360°, around a central point or axis on a colour wheel (Rezzouk *et al.* 2020), where an angle of 0° corresponds to red, an angle of 90° corresponds to green, and an angle of 180° corresponds to blue. Usually, leaf colour is included in the HUE range from 120° (green) to 60° (yellow). HUE is obtained as the circular mean of HUE pixel values inside the plant region, computed as:

$$\mathrm{HUE} = \frac{\sum_1^n \mathrm{PHV}}{\mathrm{n}} \quad (3)$$

where PHV is a single HUE pixel value and *n* is the pixel number inside the plant region.

Peroxidase activity assay

Peroxidase (POD) activity was assayed in fresh leaves collected from three NS and S plants of the BR ecotype. The extraction protocol, described in Spanò *et al.* (2023), allows recovery of total soluble (TSP) and cell-wall bound (CWP) proteins. The concentrations of proteins in the two extracts were estimated using the Bradford assay and a Bio-Rad protein assay dye reagent (Bio-Rad Laboratories, CA, USA) following the manufacturer's instructions. Protein extracts from S and NS plants were brought to a final concentration of 30 and 5 µg for TSP and CWP fractions, respectively, in a total volume of 100 µl. TSP and CWP proteins were separated by native Polyacrylamide Gel Electrophoresis (PAGE) according to Spanò *et al.* (2023) on a vertical gel apparatus (Bio-Rad Laboratories). After the electrophoretic run, POD activity in the gels was stained at room temperature for 5 min with 100 mM Tris-acetate buffer, pH 5, 1 mM metoxynaphthol and 0.15 of hydrogen peroxide (H_2O_2), according to Ferrer *et al.* (1990) and López-Serrano *et al.* (2004). The colorimetric reaction was stopped with distilled water and quantitative densitometric analyses of bands evaluated using ImageJ software (https://imagej.nih.gov/ij/; Rasband, 1997–2018).

The POD activity in TSP and CWP extracts was also spectrophotometrically evaluated at 652 nm, oxidation of 0.2 mM 3,3′,5,5′-tetramethylbenzidine (TMB) by 25 µg protein resuspended in 100 mM Tris-acetate buffer, pH 5 (pH 6.0) and 0.1 mM H_2O. POD activity was calculated using an extinction coefficient of 26.9 $mM^{-1} \cdot cm^{-1}$ and expressed as nmoles TMB oxidized $min^{-1} \cdot mg^{-1}$ protein (nmol TMBox·$min^{-1} \cdot mg^{-1}$·prot).

Lignin content analysis

Lignin content in extracts from NS and S plants was determined spectrophotometrically at 280 nm by measuring thioglycolic lignin obtained from 1 g lyophilized leaf material and resuspended in 0.5 M NaOH, following Spanò *et al.* (2023). Pure alkali lignin (Sigma-Aldrich, St. Louis, MO, USA) was used to construct the calibration curve and calculate lignin content in each sample. For this, 10 mg pure alkali lignin was subjected to the same extraction protocol and five serial 1:2 dilutions of 160 $\mu g \cdot ml^{-1}$ thioglycolic lignin resuspended in 0.5 M NaOH.

14388677, 0, Downloaded from https://onlinelibrary.wiley.com/doi/10.1111/plb.13675 by CNR Group, Wiley Online Library on [11/07/2024]. See the Terms and Conditions (https://onlinelibrary.wiley.com/terms-and-conditions) on Wiley Online Library for rules of use; OA articles are governed by the applicable Creative Commons License

Statistical analysis

Statistically significant differences at $P \leq 0.05$ were assessed with a *t*-test and ANOVA with Tukey's post-hoc test, using Statistica software, version 7.0 (Stat Soft 1984–2004, Tulsa, AZ, USA), and R software, version 4.2.1 (R Foundation for Statistical Computing, Vienna, Austria, accessed June 2022).

Principal components analysis (PCA) for the consistency of sample libraries was assessed by multivariate analysis with the chemometrics agile tool (CAT) software, version 3.1.2 (http://www.gruppochemiometria.it/index.php/software).

RESULTS

Features comparison of sanitized and non-sanitized 'Brindisino'

The open-field comparative trial showed remarkable differences in agronomic traits of S and NS BR ecotypes. Those obtained by *in vitro* meristem tip culture and thermotherapy had increased vigour (Fig. 1a) and size of capitula (Fig. 1b) compared to the NS counterpart.

The reproductive cycle ranged from 8 to 10 months, with production of the oval central flower head starting in November, followed by differentiation of three to four lateral shoots and about four lateral heads on the main stem. Although both S and NS BR ecotypes had similar plant heights (about 83 cm), S ecotype had a leaf length of 98 cm and plant diameter of 160 cm, which are higher than in the NS ecotype, with a leaf length of 85 cm and diameter of 138 cm. Other major differences between S and NS BR ecotypes were central flower head diameter and weight. S flower head diameter was 8 cm and weighed 190 g, which is 1.5- and 1.8-fold higher than in NS. No other morphological parameters among NS and S BR ecotypes differed significantly.

Assessment of phytosanitary status

Simultaneous detection of ten artichoke viruses by dot-blot hybridization from NS and S plants revealed the presence of viral infections in NS, while S plants were virus-free (Fig. 2a). High-throughput sequencing of three RNA artichoke preparations confirmed the absence of any virus infections in S plants but presence in virus genomes of NS plants. In all the three samples from NS plants, a mean of 124 reads mapped on the TMV genome sequence, with a coverage of 2.83-fold (Fig. 2b). In two of the three samples from NS, a mean of 116 reads mapped on the ArLV genome with cover of 2.79-fold (Fig. 2c). Moreover, RNAseq analysis also detected AILV infection in NS plants (Fig. 2d) which preferentially targeted the coat protein gene region of the RNA2 segment of the AILV genome, with a mean cover of 7.9e+04 fold. Only a few reads mapped on the replicase (RdRp) gene region of RNA1 of AILV, with mean cover of 996-fold. High-throughput sequencing results were validated by PCR, showing the presence of virus infections in all samples from NS, but no amplification products in samples from S plants with AILV, ArLV or TMV specific primer pairs.

Comparative analysis of whole-transcriptome Brindisino artichokes

Total RNA extracted from three samples each of S and NS plants and used for RNA sequencing on the Illumina platform. BR-S and BR-NS sequencing produced an average of 190 million reads (2 × 150 bp), with a mean of 35.6 (minimum reference value of 30) and mean yield of 56 G bases. Reads were aligned on the *C. cardunculus* reference genome, with a mean of 80% of total reads mapped. Normalized count data were used to calculate the variance stabilizing transformation (VST) from the fitted dispersion-mean relationship and clustering of samples (Figure S1a). A PCA of VST matrix samples in the sub-space PC1 *vs* PC2 (accounting 97.1% and 1.9% of total variance, respectively) showed clear separation between S and NS plants (Figure S1b), validating the consistency of the analysed libraries. Reads mapped were used to analyse DEGs in S samples compared with transcript levels of NS samples. There were 11825 DEGs with an FDR 0.05, corresponding to 44.6% of the 26,505 total *C. cardunculus* genes. Of these, 24% showed a $\log_2FC \leq -1$ (2841 DEGs) and were downregulated, whereas 19.7% were upregulated with a $\log_2FC \geq 1$ (2329 DEGs), corresponding to a total of 5170 DEGs.

A functional enrichment analysis to detect statistically significantly enriched GO terms for FDR ≤ 0.05 and KEGG pathways found upregulated genes set in the Manhattan plot (Fig. 3a), with 63 GO terms involved in molecular function, 123 GO terms involved in biological processes and 23 GO terms for cellular component significantly enriched (FDR ≤ 0.05; Table S1). Analysis of downregulated gene sets (Fig. 3b) revealed 18, 57 and 2 GO terms involved in molecular function, biological processes and cellular component main categories, respectively, were significantly enriched (FDR ≤ 0.05; Table S2).

Fig. 1. Comparison of agronomic traits in sanitized (S) *vs* non-sanitized (NS) plants of Brindisino artichoke ecotype. S plants (left row) showed superior plant vigour in open-field trials (a) and a larger size capitula (b) when compared to NS plants (right row).

14388677, 0, Downloaded from https://onlinelibrary.wiley.com/doi/10.1111/plb.13675 by CNR Group, Wiley Online Library on [11/07/2024]. See the Terms and Conditions (https://onlinelibrary.wiley.com/terms-and-conditions) on Wiley Online Library for rules of use; OA articles are governed by the applicable Creative Commons License

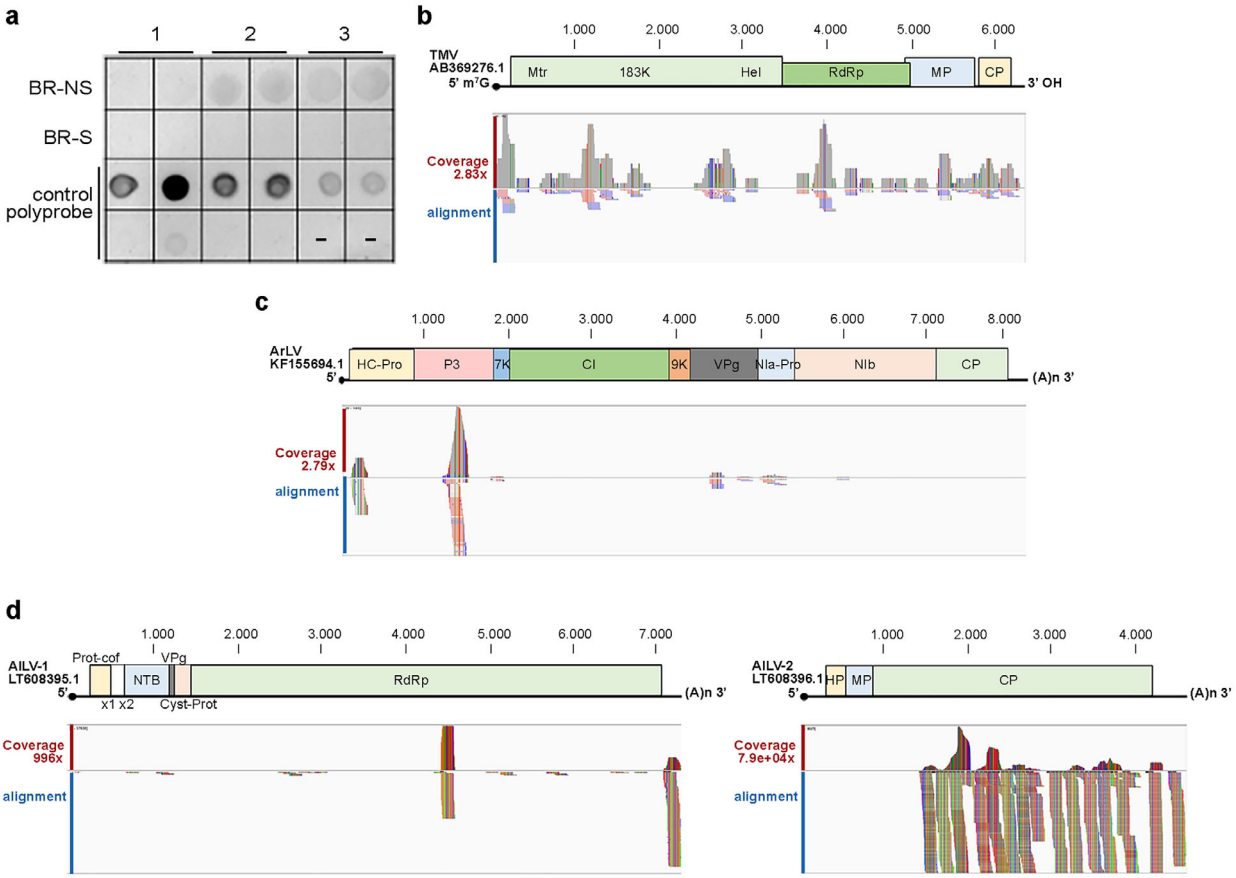

Fig. 2. Virus detection in three samples of the Brindisino (BR) ecotype collected from sanitized (S) and non-sanitized (NS) plants. (a) Dot-blot hybridization using a specific digoxigenin-labelled DNA polyprobe for the simultaneous detection of ten artichoke viruses (Minutillo *et al*. 2021). Leaf extract of healthy plant (−) and five dilutions (1:5) of 1 ng unlabelled target polyprobe sequence (+) were used as controls. Hybridization signals were displayed using the Quantity One software (Bio-Rad Laboratories). Alignment and coverage analysis of reads from one of the three BR-NS libraries against (b) tobacco mosaic virus (TMV) RNA genome, (c) artichoke latent virus (ArLV) RNA genome and (d) artichoke Italian latent virus (AILV) RNA1 and RNA2 sequences displayed using the Integrative Genomics Viewer (IGV) tool.

A general overview found that upregulated DEGs were involved in tubulin and cytoskeletal binding/motor activity related to regulation of cell cycle and division processes. Upregulated DEGs were also involved in small molecule/ion/organic compound binding and cellular response to stimulus/stress. Downregulated DEGs were involved in DNA transcription binding/activity and gene expression processes. Other downregulated DEGs were involved in regulation of organic cyclic compound biosynthesis, phenylpropanoid metabolic process and oxidoreductase activity, as well as in response to hormone stimulus and oxygen-containing compounds.

The close relationship of DEGs between each GO main categories was analysed using a Venn diagram. There were 1040 upregulated and 812 downregulated genes in the biological process main category, 927 upregulated and 627 downregulated in the molecular function main category, whereas 405 upregulated and 393 downregulated genes were in the cellular component category (Fig. 4). Of these, 170 upregulated and 252 downregulated DEGs (in green intersection) were common between these three GO main categories.

BlastKOALA tool (https://www.kegg.jp/blastkoala/) was used for a further functional characterization of upregulated and downregulated DEGs selected from GO enrichment analysis (Fig. 5). KEGG orthology (KO) analysis showed that most genes that were upregulated are involved in metabolic processes, particularly in metabolism of carbohydrates, amino acids and lipids, as well as in metabolism of cofactors, vitamins and other secondary metabolites. A similar number of up- and downregulated DEGs was observed for the energy, nucleotide, amino acid, glycan, cofactors, terpenoids and polyketides, and other secondary metabolisms, whereas the other metabolic processes were mostly downregulated. Analysis of genetic information processing pathways showed upregulation of genes related to translation, folding, sorting and degradation, whereas in the transcription pathway there were a high number of downregulated DEGs. A significant high number of upregulated DEGs weere involved in replication and repair processes, whereas another high number of DEGs, both up- and downregulated, were involved in environmental information processing, with >20 KO entry pathways related to signal transduction, compared to membrane transport pathways. Finally, there was a general upregulation of pathways involved in cellular processes, whereas processes for environmental adaptation systems were more markedly downregulated.

14388677, 0, Downloaded from https://onlinelibrary.wiley.com/doi/10.1111/plb.13675 by CNR Group, Wiley Online Library on [11/07/2024]. See the Terms and Conditions (https://onlinelibrary.wiley.com/terms-and-conditions) on Wiley Online Library for rules of use; OA articles are governed by the applicable Creative Commons License

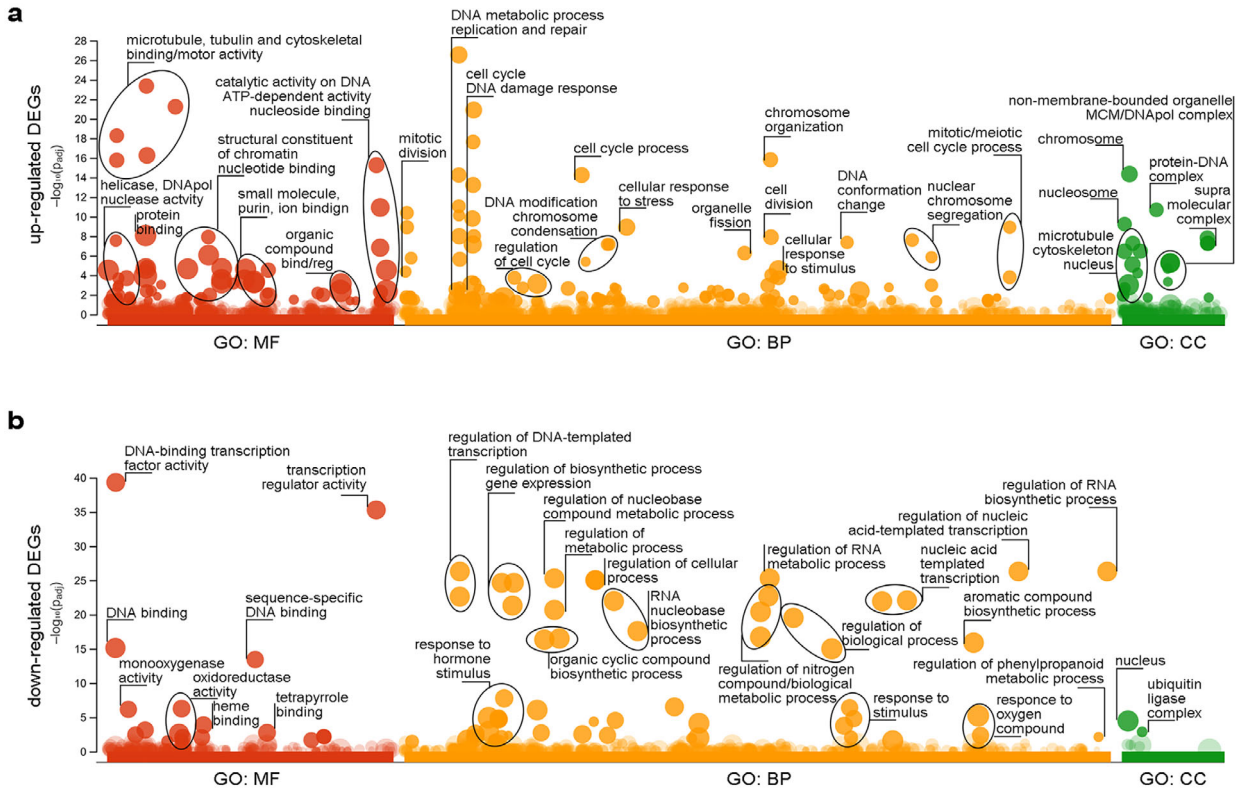

Fig. 3. Functional enrichment analysis of (a) upregulated and (b) downregulated DEGs obtained from RNAseq differential expression analysis performed with g:GOSt tool on the g:Prifiler2 web server (https://biit.cs.ut.ee/gprofiler/gost, v. *e109_eg56_p17*_1d3191d, accessed June 2023). Differentially expressed genes (DEGs) were separated in three Gene Ontology (GO) main categories: molecular function (MF), biological process (BP) and cellular component (CC). Circle sizes in the Manhattan plot correspond to number of genes annotated in each specific GO term. Circles located close together on the *x*-axis correspond to related GO subtree. Negative log10 of $P \leq 0.05$ adjusted for multiple testing with the Benjamini-Hochberg procedure, which controls false discovery rate (FDR), was used to display significantly enriched GO terms. Light coloured circles represent non-significant GO terms.

High-throughput plant phenotyping

Both S and NS plants were used for phenotyping to detect agronomic and physiological differences between them. A daily RH maximum (RHmax) of 85% and daily RH minimum (RHmin) of 45% were recorded. Temperature had a daily Tmax of 29 °C and daily Tmin of 2 °C. During each acquisition, the high-throughput plant phenotyping platform collected 340 Mb of data, consisting of 325 phenotyping images.

The data described greater growth dynamics for S compared to NS plants. Leaf morphology and size analysis of projected shoot area (Fig. 6a) revealed a faster linear increase in growth of S compared to NS plants. This increase in size of S plants was also observed in plant height measured in the two conditions (Fig. 6b). There was an increase in circumference of about 2.5-fold for S compared to NS plants. Similar results were also obtained for solidity from a top view (Fig. 6c). Interestingly, the analyses highlighted inversion of the solidity trait, with a marked initial lower solidity of S plants, that was overturned by the end of the experiment. During the first week, S plant solidity increased while that of NS plants decreased. Analysis of plant water content in the near-infrared showed a higher water content in S than in NS plants (Fig. 6d). Notably, these data were positively correlated with the different water content of leaves of S plants compared to NS plants in freeze-dried fresh plant material collected at the end of each phenotype sampling (Figure S2). Analysis of the Senescence Index (Fig. 6e) found similar values for both conditions at the beginning of the experiment, followed by an increase in senescence processes at the third and fourth sampling, which was larger for S plants. The result was similar from analysis of the HUE index circular mean top view of leaves, which showed an increase in yellowing processes at the final sampling in both S and NS plants (Fig. 6f).

Peroxidase activity and lignin accumulation in artichoke

The POD enzymes are bifunctional and can function in H_2O_2 scavenging, oxidizing various substrates, as well as in production of reactive oxygen species (ROS), being involved in both developmental processes and in response to biotic and abiotic stress (Kidwai *et al.* 2020). POD activity was evaluated in S and NS artichoke plants using *in gel* assay and spectrophotometry (Fig. 7). *In gel* POD activity of total soluble protein and cell wall-bound protein extracts showed higher levels in S compared to NS samples. Coomassie brilliant blue staining confirmed the equal gel loading. Moreover, POD activity in cell wall-bound protein was significantly higher than in total soluble protein extracts. Indeed, for native PAGE, POD activity was detected with only 5 µg cell wall-bound protein extract

14388677, 0, Downloaded from https://onlinelibrary.wiley.com/doi/10.1111/plb.13675 by CNR Group, Wiley Online Library on [11/07/2024]. See the Terms and Conditions (https://onlinelibrary.wiley.com/terms-and-conditions) on Wiley Online Library for rules of use; OA articles are governed by the applicable Creative Commons License

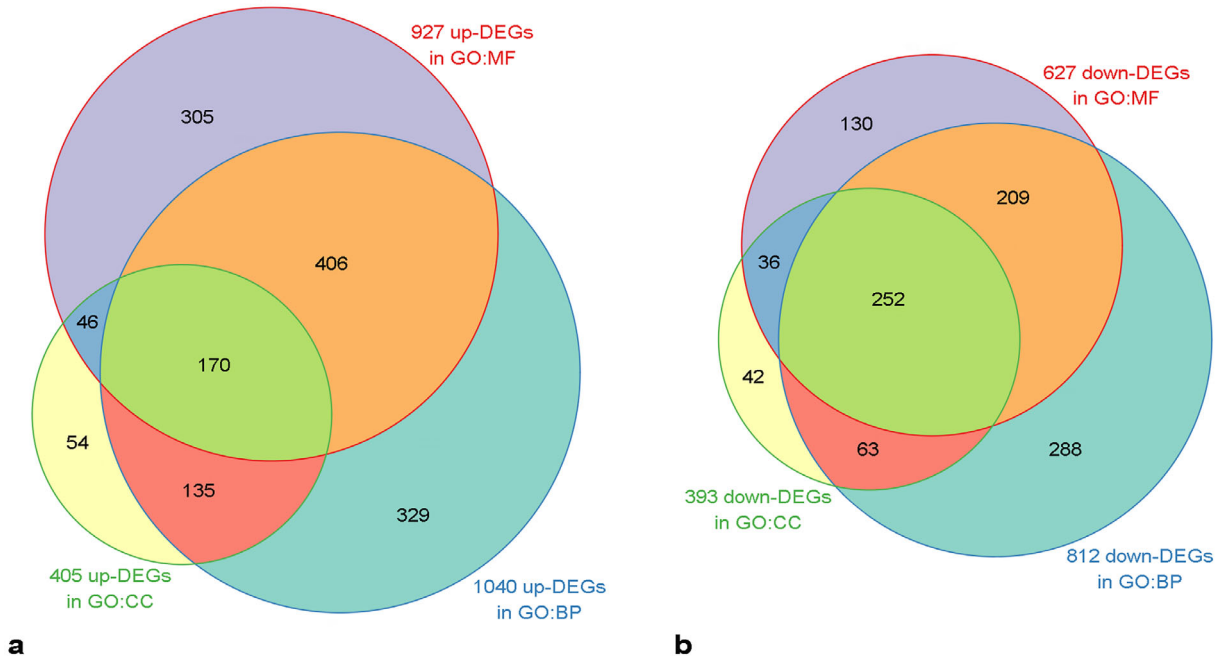

Fig. 4. Venn diagram relationships analysis among the three Gene Ontology (GO) main categories: molecular function (MF), biological process (BP) and cellular component (CC) (a) of upregulated differentially expressed genes (DEGs) and (b) downregulated DEGs selected from GO enrichment analysis.

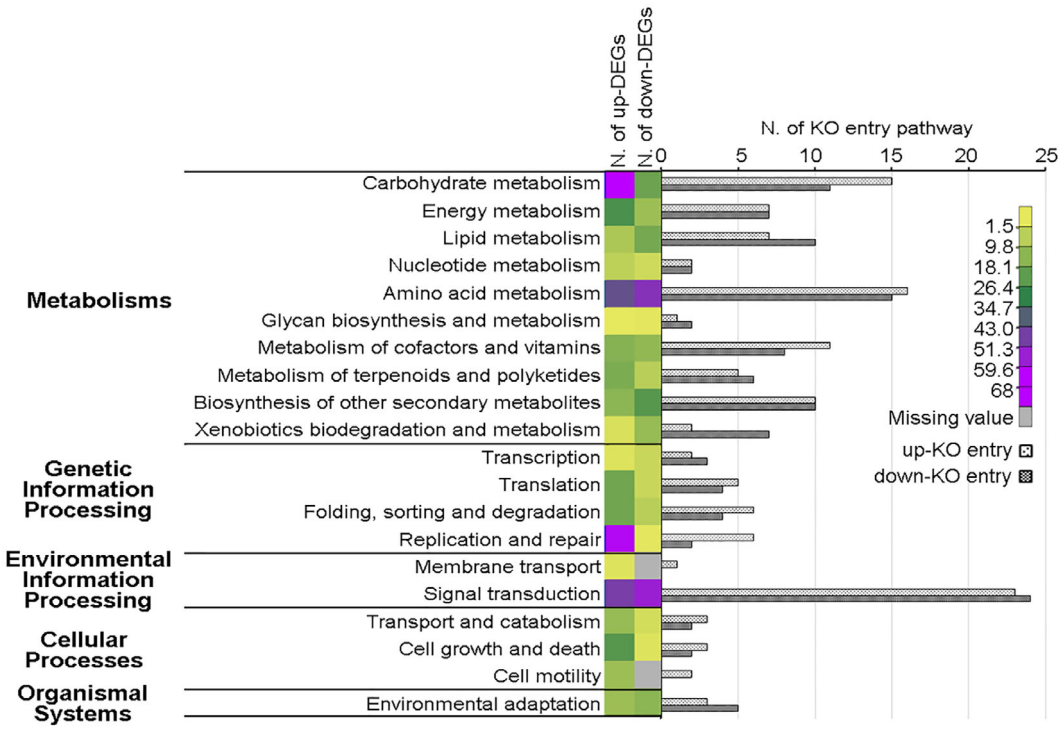

Fig. 5. Functional classification of upregulated and downregulated differentially expressed genes (DEGs) in sanitized (S) *vs* non-sanitized (NS) BR plants based on the number of DEGs for each KEGG orthology (KO) entry and KO pathways analysed.

compared to the 30 μg total soluble protein extract loaded on the gel, both for S and NS plants. The results of *in gel* activity were validated by the spectrophotometric assay, which confirmed the higher POD activity of cell wall-bound protein extracts compared to the total soluble protein fraction, as well as an increase of 3.5-fold in total soluble proteins (Fig. 7a) and 4.7-fold in cell wall-bound proteins (Fig. 7b) in S compared to NS plants.

14388677, 0, Downloaded from https://onlinelibrary.wiley.com/doi/10.1111/plb.13675 by CNR Group, Wiley Online Library on [11/07/2024]. See the Terms and Conditions (https://onlinelibrary.wiley.com/terms-and-conditions) on Wiley Online Library for rules of use; OA articles are governed by the applicable Creative Commons License

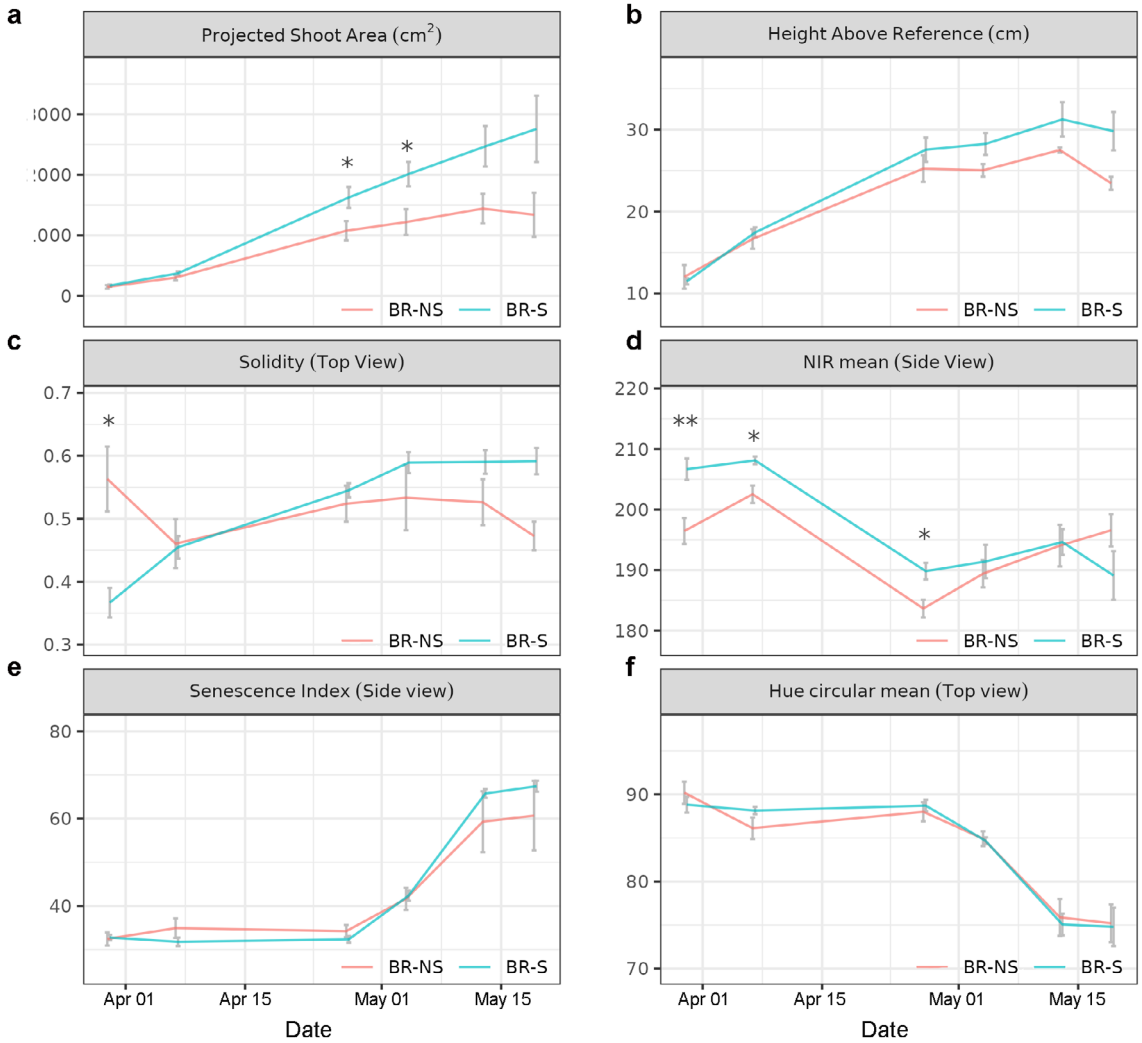

Fig. 6. High-throughput plant phenotyping of sanitized (S) *vs* non-sanitized (NS) BR plants. Images were acquired in the RGB spectral range in top view above the plant and from the side view. Pixel values were computed to obtain the following optical indices: projected shoot area (PSA); height above reference; solidity; NIR mean; senescence index (SI); and HUE circular mean. Six plants for each sanitization condition were measured within 2 months (from April to May 2022). Asterisk (*) indicates significant differences obtained by *t*-test for each value–treatment effect between BR-NS and BR-S, at each time of sampling (*t*-test values are reported in Table S3).

To verify the potential role of increased cell wall-bound protein in cell wall stiffening through POD involvement in lignin biosynthesis, the lignin content was measured in S and NS plants in the same conditions tested during phenotyping. A calibration curve ($y = 0.0071x - 0.0115$; $R^2 = 0.99$) was used to estimate the concentration of thioglycolic lignin formed. There was no statistically significant difference between S and NS plants during this time course, whereas for both conditions there was a slight increase of lignin content over time, being 1.5-fold from the first to the last collection point (Fig. 8).

DISCUSSION

Evaluation of biodiversity in Italy ensures the conservation and sustainable use of the diverse biological resources and ecosystems. Plant biodiversity is often threatened by the occurrence of viral infections, against which no efficient control measures are available (Gallitelli *et al.* 2012). The increased transmission and accumulation of pathogens, often in mixed infection, is mainly related to clonal propagation of plants of unknown phytosanitary status. To avoid phytosanitary risks and loss of biodiversity from these routine agronomic techniques, the use of virus-free plant material is emphasized. A sanitation protocol based on a combination of *in vitro* meristem tip culture and thermotherapy has now been adopted to produce virus-free globe artichoke cultivated germplasm (Spanò *et al.* 2018). Evaluation of agronomic traits of the S BR ecotype in open-field trials showed overall increased performance of this plant after sanitation (Fig. 1). The harvested capitula for human consumption had improved qualitative and quantitative traits (Fig. 1b) increasing their demand by farmers for new plantings. Between 2015 and 2019, over one million virus-free and true-to-type 'basic' artichoke category with protected roots have been marketed, with an average of 200,000 plants·year^{-1}. The demand came mainly from farmers in southern Italy, in regions traditionally suited to cultivation of this crop, such as

Plant Biology © 2024 The Author(s). *Plant Biology* published by John Wiley & Sons Ltd on behalf of German Society for Plant Sciences, Royal Botanical Society of the Netherlands.

14388677, 0, Downloaded from https://onlinelibrary.wiley.com/doi/10.1111/plb.13675 by CNR Group, Wiley Online Library on [11/07/2024]. See the Terms and Conditions (https://onlinelibrary.wiley.com/terms-and-conditions) on Wiley Online Library for rules of use; OA articles are governed by the applicable Creative Commons License

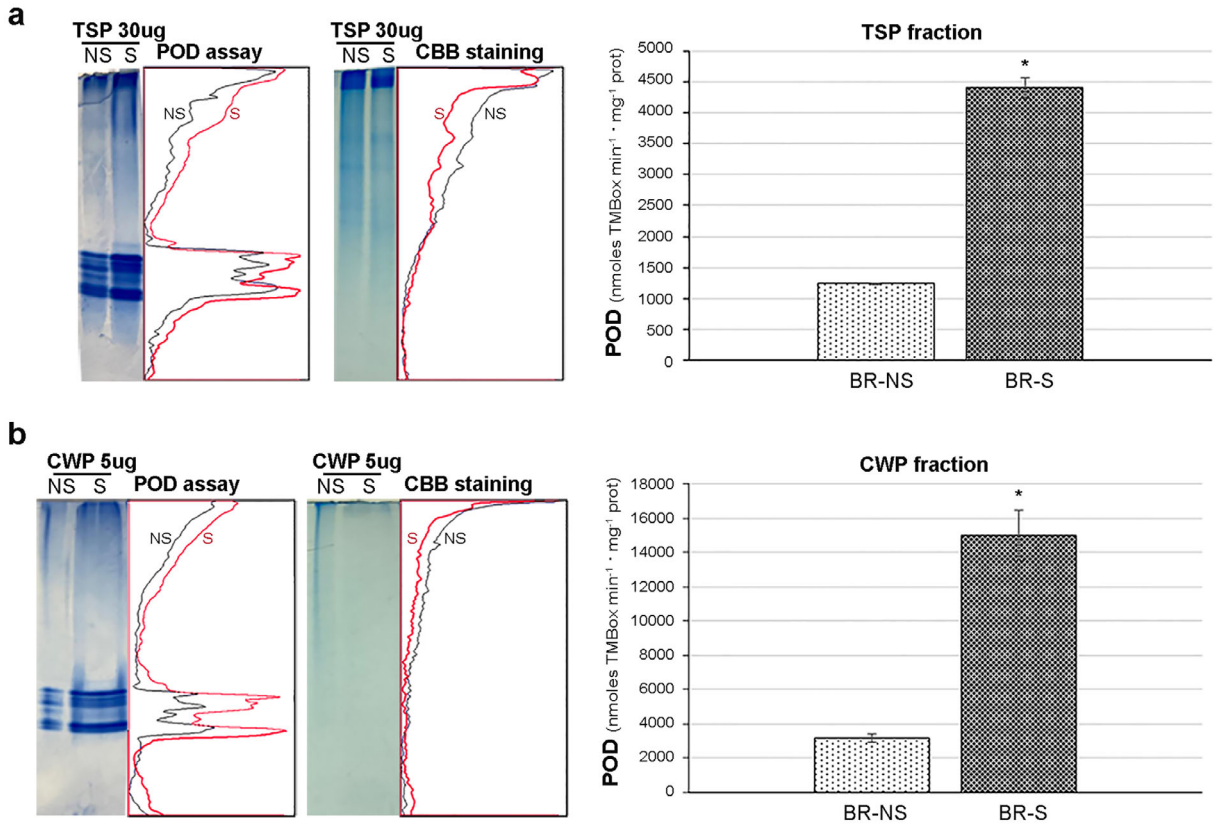

Fig. 7. Analysis of peroxidase (POD) activity in artichoke samples. Representative image from three independent experiments of native Polyacrylamide Gel Electrophoresis of (a) 30 μg soluble (TSP) and (b) 5 μg cell wall (CWP) protein fractions extracted from Brindisino (BR) plants, in non-sanitized (NS) and sanitized (S) conditions. Coomassie Brilliant Blue (CBB) staining was used to assess equal gel loading. Quantification of *in gel* POD activity of NS (black profile) and S (red profile) plants was performed with ImageJ software. Histogram shows the spectrophotometric POD activity of TSP and CWP extracts obtained from NS and S plants. Values represent mean ± SE of three biological replicates, each in triplicate. Asterisk (*) indicates significant differences obtained by *t*-test for two independent group in (a) TSP fraction between BR-NS [mean (M) = 1238.2, ±SD = 33.1] and BR-S [M = 4402.2, ±SD = 212.7] for $t(8) = -32.8$, $P < 0.0001$]; and in (b) CWP fraction between BR-NS [M = 3183.3, ±SD = 506.8] and BR-S [M = 14975.3, ±SD = 2063.4] for $t(6) = -11.1$, $P < 0.0001$].

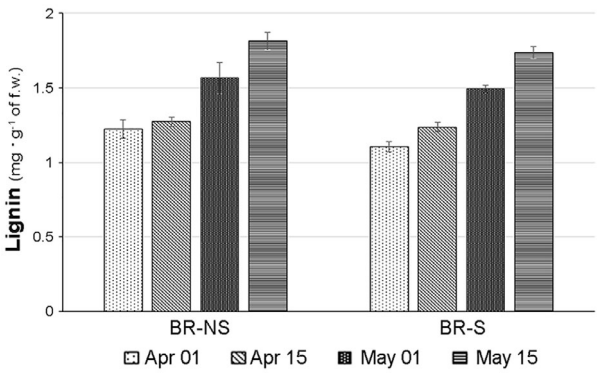

Fig. 8. Analysis of lignin content in sanitized (S) and non-sanitized (NS) Brindisino (BR) artichoke plants collected during phenotyping experiment. No statistically significant differences were observed after a two-way ANOVA post-hoc Tukey HSD test for homogeneous groups ($P \leq 0.05$).

Apulia, Sicily, Sardinia, Calabria and Basilicata (FreshPlaza 2020). Moreover, the use of certified plants allowed compliance with guidelines of Current EU Directives 93/61/CEE and 93/62/CEE, as modified/adapted by the new Plant Health Regulation (EU) 2016/2031 and (EU) 2017/625 (Barba *et al.* 2004; Papanice *et al.* 2004; Spanò *et al.* 2018). The decrease in yield and delayed harvesting time for NS BR ecotype compared to S ecotype is associated with the occurrence of infectious pathogens. Analysis of phytosanitary status revealed the presence of viral infections in the NS BR ecotype, as previously reported also for other Apulian ecotypes (Gallitelli *et al.* 2004; Minutillo *et al.* 2015; Spanò *et al.* 2018, 2023). The artichoke Italian latent virus (AILV) is a nepovirus transmitted by nematodes and therefore characterized by slow spread through the soil. This virus can also infect meristem tips and be seed-transmitted, increasing its diffusion in the Mediterranean Basin (Kyriakopoulou 1995; Gallitelli *et al.* 2004; Salleh *et al.* 2017). The current incidence of AILV infection is probably related to vegetative transmission in BR-NS plants and suggests increased use of sanitized material in the new plantings. Artichoke latent virus (ArLV) is a macluravirus transmitted by aphids with a non-persistent modality, making it the most widespread among the viruses that infect globe artichoke and highlighting the need to better control the vector to reduce the incidence of virus spread (Gallitelli *et al.* 2004). Both AILV and ArLV infections are usually symptomless, but their presence has a damaging effect on crop production

14388677, 0, Downloaded from https://onlinelibrary.wiley.com/doi/10.1111/plb.13675 by CNR Group, Wiley Online Library on [11/07/2024]. See the Terms and Conditions (https://onlinelibrary.wiley.com/terms-and-conditions) on Wiley Online Library for rules of use; OA articles are governed by the applicable Creative Commons License

associated with a lower stress tolerance. Tobacco mosaic virus (TMV) is transmitted by contact, and the presence of the virus in artichoke plants is mainly associated with bad agricultural practices.

Plant genotype, environmental growth conditions, or presence of pathogen infections, will result in different artichoke culture outcomes (Tanner *et al.* 2022). In this study, we analysed the transcriptomic profile of the BR ecotype, one of the most cultivated artichokes in the Apulian region, in S *vs* NS plants. A total of 5170 genes, up- and downregulated, were differentially expressed (Figs 3 and 4) between S and NS plants. Most genes were involved in biological processes, although the same genes code for proteins related to molecular function or cellular component, or both. Similarly, many DEGs are involved in molecular function, but at the same time express proteins linked to biological process or cellular component main categories. The overall analysis of gene functions highlights modulation of genes that control growth processes, regulation of gene expression, response to stress and signalling molecules. The comparison between S and NS plants highlights many DEGs involved in the strong modulation of signal transduction (Fig. 5), as also observed in previous studies (Spanò *et al.* 2023). This also explains the different modulation of metabolism of cofactors and vitamins, terpenoids and polyketides and secondary metabolites between S and NS plants. After a virus enters the cell, signalling pathways are activated by phytohormones whose sophisticated crosstalk facilitates a balanced response to abiotic and biotic stresses (Slavokhotova *et al.* 2021). Activation of defence mechanisms modulates expression of many other genes involved in information processing (Alexander & Cilia 2016), as also reported in this study (Figs 3 and 5).

The differential regulation of genes and related proteins during viral infection highlights the continuous plant–pathogen challenge and includes many visible physiological changes, based on primary metabolism disturbance, as well as thermal energy dissipation (Fig. 5), and symptoms of the plant disease (Tanner *et al.* 2022). Moreover, a pathogen may affect photosynthetic performance and source–sink relations (Venturini *et al.* 2016; Zanini *et al.* 2020). In fact, in infected source leaves, photosynthesis is reduced, with a decrease in starch accumulation in cells and accumulation of soluble sugars in the phloem (Shalitin & Wolf 2000). The altered level of carbohydrates in infected plants is accompanied by an increase in respiration and a reduction in plant development. This could explain the reduced vigour of naturally virus-infected NS artichoke compared to S plants in open field conditions (Fig. 1) and the corresponding modulation of DEGs involved in carbohydrate metabolism (Fig. 5).

Results from high-throughput plant phenotyping experiments correlated with transcriptome changes detected between S *vs* NS plants. The increase in biomass of S is mainly related to a boost in volume, leaf area and photosynthetic activity in S compared to NS plants (Fig. 6), as observed at molecular level. However, the rapid development of S plants in pots, which were too small in relation to the total plant biomass, was accompanied by intensification of senescence and yellowing processes at the end of the phenotyping experiment. Precisely evaluation of some digital indices, like projected shoot area, height above reference and solidity projected shoot area, should be considered as potential parameters for detection of viral disease or abiotic stresses after transplanting in open fields and for improving qualitative and quantitative traits of S plants.

However, plant–virus interaction occurs at multiple levels and many other DEGs are also up- and downregulated. Regarding lipid metabolism, RNAseq results showed a different modulation of related genes in S compared to NS plants. Lipids are the main structural components of biological membranes, contributing to their fluidity and integrity, as well as being involved in the photosynthetic processes, energy storage, signalling and metabolites traffic regulation through cell membranes (Mehta *et al.* 2021), therefore continuously remodelled during stress conditions and plant development (Yang & Benning 2018). The modulation of amino acid metabolism may be related to alterations to key proteins abundance involved in carbon fixation (Lehrer & Komor 2009), photosynthetic electron transport chain (Souza *et al.* 2019; Zanini *et al.* 2021), synthesis of defence responses (Zeier 2013; Alexander & Cilia 2016), redox state through the production/scavenging of ROS (Rodríguez *et al.* 2010).

Peroxidase (POD) enzymes are largely implicated in the generation of ROS during pathogen defence but are also known to be involved in detoxification of H_2O_2, controlling ROS levels inside cells (Bauer 2000; Alexander & Cilia 2016). Moreover, PODs are involved in the strengthening and/or loosening of cell walls, being associated with growth restriction and/or cell elongation (Passardi *et al.* 2004). Cell wall strengthening depends on cross-linking of polysaccharide-linked ferulates, extensions and lignin monomers, through the peroxidative cycle of POD. Since analysis of lignin content showed no statistically significant difference in this polymer in S and NS artichokes (Fig. 8), the higher POD activity in S plants (Fig. 7) cannot be related to higher cell wall stiffening. On the other hand, enhanced POD activity in S artichokes could be associated with increased cell wall loosening through generation of OH radicals in the hydroxylic cycle and the action of auxins that promote cell elongation and plant growth (Passardi *et al.* 2004). Therefore, the increase in POD activity seems mostly related to a novel attribute of S plants, probably acquired by meristem tip culture and *in vitro* thermotherapy. It is also important to consider that the increase of PODs in S plants makes them potentially more resistant to biotic and abiotic stresses (Kidwai *et al.* 2020). Plant tissue culture is widely used in agriculture to overcome difficulties in crop propagation and solve phytosanitary problems in mother plant material, but it has long been known that *in vitro* conditions may induce genotypic and phenotypic modifications. Variation in DNA methylation patterns seem to be directly implicated in these modifications (Miguel & Marum 2011), as a result of highly dynamic mechanisms of chromatin remodelling occurring during cell de-differentiation and differentiation processes in *in vitro* cultured plants. In these plants, epigenetic variation reflects the adaptation to a new environment, which includes response to signals that may trigger different plant development capacity, influencing gene transcription in response to different stimuli, such as stress, pathogen infection, light, and hormones (Kidwai *et al.* 2020).

Overall, morphological differences between S and NS plants derive mainly from alterations in plantlet photosystem and signal transduction ability acquired during plant tissue culture. A more complete understanding of the viral infection impact on

Plant Biology © 2024 The Author(s). *Plant Biology* published by John Wiley & Sons Ltd on behalf of German Society for Plant Sciences, Royal Botanical Society of the Netherlands.

14388677, 0, Downloaded from https://onlinelibrary.wiley.com/doi/10.1111/plb.13675 by CNR Group, Wiley Online Library on [11/07/2024]. See the Terms and Conditions (https://onlinelibrary.wiley.com/terms-and-conditions) on Wiley Online Library for rules of use; OA articles are governed by the applicable Creative Commons License

artichoke plant growth will be elucidated through analysing the transcriptome profile, carbon flux in source leaves, and accumulation of photosynthetic metabolites in S plants subjected to viral infection through rub-inoculation under controlled conditions.

CONCLUSION

The availability of virus-free and true-to-type certified stocks of artichoke has allowed the recovery of ecotypes at risk of erosion and has enriched the overall biodiversity of Apulian horticultural species. Virus-free material provides a range of benefits to plant growers, including enhanced disease resistance, improved yield, reduced crop losses, sustainability advantages, prevention of viral spread, and increased marketability of the final produce. The growing interest among farmers of S plants promotes the return of this crop to traditionally cultivated artichoke areas.

Differential gene expression analysis can help to identify genes that are up- or downregulated in response to specific treatments or stressors and analyse physiological activities significantly affecting development and growth of S artichoke plants. But analysis of large datasets to understand the plant–pathogen–environment interaction constitutes one of the most important challenges of the '-omic' era. Therefore, by combining plant transcriptome and phenotyping results, we focused on factors that highlight significant differences in metabolic pathways of S plants compared to the NS plants. Moreover, this study opens new perspectives to detect and quantify plant disease symptoms using non-invasive sensor technology, like plant phenotyping, which represents a promising technique for the early diagnosis of disease in open-field conditions, and in biofuel research to assess crop biomass with reduced lignin content.

AUTHOR CONTRIBUTIONS

Conceptualization, R.S. and T.M.; methodology, R.S., M.C.d.P., F.C. and T.M.; validation, R.S., A.P., S.S. and S.F.; formal analysis, R.S., A.P., S.S., S.F., M.C.d.P., F.C. and T.M.; investigation, R.S., A.P., S.S. and S.F.; data curation, R.S., A.P., S.S. and S.F.; writing–original draft preparation, R.S.; writing–review and editing, R.S., A.P., S.S., S.F., M.C.d.P., F.C. and T.M.

ACKNOWLEDGEMENTS

We are grateful to Prof. Donato Gallitelli, University of Bari, for his helpful support in the experimental design of the research project, critical comments on the results, and review of the manuscript. This work was supported by REGIONE PUGLIA: CUP: H94I20000410008: Research for Innovation (REFIN) – 6E389E5E: Intervento cofinanziato dall'Unione Europea a valere sul POR Puglia 2014–2020, Asse Prioritario OT X "Investire nell'istruzione, nella formazione e nella formazione professionale per le competenze e l'apprendimento permanente"–Azione 10.4–project "Caratterizzazione di geni coinvolti nella sintesi di composti secondari di interesse salutistico e industriale in ecotipi locali di carciofo risanato (ERiCa)"; REGIONE BASILICATA: DGR. N. 402 del 28/06/2019: CUP: G89J19001000003: SiFESR-15/2019/0209 Progetto PHENO-LAB 4.0 – "PO FESR Basilicata 2014-2020 – Azione 1A.1.5.1. Avviso per il sostegno a progetti di rafforzamento e ampliamento delle Infrastrutture di Ricerca inserite nel Piano Triennale delle Infrastrutture di Ricerca della Regione Basilicata." – Area di specializzazione: BIOECONOMIA; Agritech National Research Center and received funding from the European Union Next-GenerationEU: PIANO NAZIONALE DI RIPRESA E RESILIENZA (PNRR) – MISSIONE 4 COMPONENTE 2, INVESTIMENTO 1.4 – D.D. 1032 17/06/2022: CN00000022 – The manuscript reflects only the authors' views and opinions, neither the European Union nor the European Commission can be considered responsible for them.

CONFLICT OF INTEREST

The authors declare no conflict of interest.

DATA AVAILABILITY STATEMENT

RNAseq data: Spanò R.; 2023; Artichoke transcriptome; NCBI data repository; Bioproject ID number PRJNA1034968.

SUPPORTING INFORMATION

Additional supporting information may be found online in the Supporting Information section at the end of the article.

Figure S1. Analysis of consistency of RNAseq libraries by (a) sample-to-sample distances heatmap calculated from the variance-stabilizing transformation (VST) of normalized count data for overall gene expression. Clustering of Brindisino (BR) sanitized (S) and non-sanitized (NS) plants is expressed by the intensity of square colours. (b) Principal components analysis (PCA) score plot showing variance among the three biological replicates for S and NS conditions. On each axis is shown percentages of variation explained by the principal components.

Figure S2. Analysis of weight losses (expressed in percentage) in sanitized (S) leaves compared to non-sanitized (NS) Brindisino (BR) plants observed after freeze-drying of fresh plant material collected at the end of each phenotyping sampling. On *x*-axis is the time course of sampling.

Table S1. Gene ontology (GO) terms significantly enriched for FDR ≤ 0.05 and relatives upregulated DEGs.

Table S2. Gene ontology (GO) terms significantly enriched for FDR ≤ 0.05 and relatives downregulated DEGs.

Table S3. Analysis of high-throughput plant phenotyping statistically significant differences between non-sanitized (NS) and sanitized (S) plants at each time of sampling by *t*-test.

REFERENCES

Alexander M.M., Cilia M. (2016) A molecular tug-of-war: global plant proteome changes during viral infection. *Current Plant Biology*, **5**, 13–24.

Aydoğdu M., Kurbetli İ., Ozan S. (2016) First report of *Sclerotium rolfsii* causing crown rot on globe artichoke in Turkey. *Plant Disease*, **100**, 2161.

Barba M., Di Lernia G., Babes G., Citrulli F. (2004) Produzione e conservazione di germoplasma di carciofo di tipo 'Romanesco' esente da virus. *Italus Hortus*, **11**, 5–10.

Barnett O. (1986) Surveying for plant viruses: design and consideration. In: Campbell C.L., Madden L.V. (Eds), *Introduction to plant disease epidemiology*.

14388677, 0, Downloaded from https://onlinelibrary.wiley.com/doi/10.1111/plb.13675 by CNR Group, Wiley Online Library on [11/07/2024]. See the Terms and Conditions (https://onlinelibrary.wiley.com/terms-and-conditions) on Wiley Online Library for rules of use; OA articles are governed by the applicable Creative Commons License

Wiley Interscience, New York, NY, USA, pp 147–166.
Bauer M.R. (2000) Role of reactive oxygen species and antioxidant enzymes in systemic virus infections of plants. *Journal of Phytopathology*, **148**, 297–302.
Benjamini Y., Hochberg Y. (1995) Controlling the false discovery rate, a practical and powerful approach to multiple testing. *Journal of the Royal Statistical Society: Series B: Methodological*, **57**, 89–300.
Cirulli M., Bubici G., Amenduni M., Armengol J., Berbegal M., Jiménez-Gasco M., Jiménez-Díaz R.M. (2010) *Verticillium* wilt: a threat to artichoke production. *Plant Disease*, **94**, 1176–1187.
Corda P., Fiori M., Carta C. (1982) Osservazioni sul "marciume dei capolini" del carciofo (*Cynara scolymus* L.) da *Botrytis cinerea* Pers. in Sardegna. *Studi Sassaresi. Sezione 3: Annali della Facoltà di Agraria dell'Università di Sassari*, **16**, 193–197.
Cravero V., Martin E., Cointry E. (2007) Genetic diversity in *Cynara cardunculus* determined by sequence-related amplified polymorphism markers. *Journal of the American Society for Horticultural Science*, **132**, 208–212.
Ferrer M.A., Calderón A.A., Muñoz R., Ros Barceló A. (1990) 4-methoxy-α-naphthol as a specific substrate for kinetic, zymographic and cytochemical studies on plant peroxidase activities. *Phytochemical Analysis*, **1**, 63–69.
FreshPlaza (2020) Vivaio F.lli. Corrado: continuano le innovazioni sulla propagazione dei carciofi. Available from https://www.freshplaza.it/article/9208975/vivaio-f-lli-corrado-continuano-le-innovazioni-sulla-propagazione-dei-carciofi/ (accessed June 2023).
Gallitelli D., Mascia T., Martelli G.P. (2012) Viruses in artichoke. *Advances in Virus Research*, **84**, 289–324.
Gallitelli D., Rana G.L., Vovlas C., Martelli G.P. (2004) Viruses of globe artichoke: an overview. *Journal of Plant Pathology*, **86**, 267–281.
Genangeli A., Avola G., Bindi M., Cantini C., Cellini F., Grillo S., Petrozza A., Riggi E., Ruggiero A., Summerer S., Tedeschi A., Gioli B. (2023) Low-cost hyperspectral imaging to detect drought stress in high-throughput phenotyping. *Plants*, **12**, 1730.
Golzarian M.R., Frick R.A., Rajendran K., Berger B., Roy S., Tester M., Lun D.S. (2011) Accurate inference of shoot biomass from high-throughput images of cereal plants. *Plant Methods*, **7**, 2.
Kanehisa M., Sato Y., Morishima K. (2016) BlastKOALA and GhostKOALA, KEGG tools for functional characterization of genome and metagenome sequences. *Journal of Molecular Biology*, **428**, 726–731.
Kidwai M., Ahmad I.Z., Chakrabarty D. (2020) Class III peroxidase: an indispensable enzyme for biotic/abiotic stress tolerance and a potent candidate for crop improvement. *Plant Cell Reports*, **39**, 1381–1393.
Kyriakopoulou P.E. (1995) Artichoke Italian latent virus causes artichoke patchy chlorotic stunting disease. *Annals of Applied Biology*, **127**, 489–497.
Langmead B., Salzberg S.L. (2012) Fast gapped-read alignment with Bowtie 2. *Nature Methods*, **9**, 357–359.
Langmead B., Trapnell C., Pop M., Salzberg S.L. (2009) Ultrafast and memory-efficient alignment of short DNA sequences to the human genome. *Genome Biology*, **10**, R25.
Lehrer A.T., Komor E. (2009) Carbon dioxide assimilation by virus-free sugarcane plants and by plants which were infected by sugarcane yellow leaf virus. *Physiological and Molecular Plant Pathology*, **73**, 147–153.
López-Serrano M., Fernández M.D., Pomar F., Pedreño M.A., Ros Barceló A. (2004) *Zinnia elegans* uses the same peroxidase isoenzyme complement for cell wall lignification in both single-cell tracheary elements and xylem vessels. *Journal of Experimental Botany*, **55**, 423–431.
Love M.I., Huber W., Anders S. (2014) Moderated estimation of fold change and dispersion for RNA-seq data with DESeq2. *Genome Biology*, **15**, 550.
Mehta S., Chakraborty A., Roy A., Singh I.K., Singh A. (2021) Fight hard or die trying: current status of lipid signaling during plant-pathogen interaction. *Plants*, **10**, 1098.
Miguel C., Marum L. (2011) An epigenetic view of plant cells cultured in vitro: somaclonal variation and beyond. *Journal of Experimental Botany*, **62**, 3713–3725.
Minutillo S.A., Marais A., Mascia T., Faure C., Svanella-Dumas L., Theil S., Payet A., Perennec S., Schoen L., Gallitelli D., Candresse T. (2015) Complete nucleotide sequence of artichoke latent virus shows it to be a member of the genus *Macluravirus* in the family *Potyviridae*. *Phytopathology*, **105**, 1155–1160.
Minutillo S.A., Mascia T., Gallitelli D. (2012) A DNA probe mix for the multiplex detection of ten artichoke viruses. *European Journal of Plant Pathology*, **134**, 459–465.
Minutillo S.A., Spanò R., Gallitelli D., Mascia T. (2021) Simultaneous detection of 10 viruses in globe artichoke by a synthetic oligonucleotide-based DNA polyprobe. *European Journal of Plant Pathology*, **160**, 991–997.
Papanice M.A., Campanale A., Bottalico G., Sumerano P., Gallitelli G. (2004) Produzione di germoplama risanato di carciofo brindisino. *Italus Hortus*, **11**, 11–15.
Passardi F., Penel C., Dunand C. (2004) Performing the paradoxical: how plant peroxidases modify the cell wall. *Trends in Plant Science*, **9**, 534–540.
Penalver R., Duranvila N., Lopez M.M. (1994) Characterization and pathogenicity of bacteria from shoot tips of the globe artichoke (*Cynara scolymus* L). *Annals of Applied Biology*, **125**, 501–513.
Rezzouk F.Z., Gracia-Romero A., Kefauver S.C., Gutiérrez N.A., Aranjuelo I., Serret M.D., Araus J.L. (2020) Remote sensing techniques and stable isotopes as phenotyping tools to assess wheat yield performance: effects of growing temperature and vernalization. *Plant Science*, **295**, 110281.
Robinson J.T., Thorvaldsdóttir H., Winckler W., Guttman M., Lander E.S., Getz G., Mesirov J.P. (2011) Integrative genomics viewer. *Nature Biotechnology*, **29**, 24–26.
Rodríguez M., Taleisnik E., Lenardon S., Lascano R. (2010) Are sunflower chlorotic mottle virus infection symptoms modulated by early increases in leaf sugar concentration? *Journal of Plant Physiology*, **167**, 1137–1144.
Salleh W., Minutillo S.A., Spanò R., Zammouri S., Gallitelli D., Mnari-Hattab M. (2017) Occurrence of artichoke infecting viruses in Tunisia. *EPPO Bulletin*, **47**, 48–56.
Sancho-Adamson M., Trillas M.I., Bort J., Fernandez-Gallego J.A., Romanyà J. (2019) Use of RGB vegetation indexes in assessing early effects of *Verticillium* wilt of olive in asymptomatic plants in high and low fertility scenarios. *Remote Sensing*, **11**, 607.
Shalitin D., Wolf S. (2000) Cucumber mosaic virus infection affects sugar transport in melon plants. *Plant Physiology*, **123**, 597–604.
Slavokhotova A., Korostyleva T., Shelenkov A., Pukhalskiy V., Korottseva I., Slezina M., Istomina E., Odintsova T. (2021) Transcriptomic analysis of genes involved in plant defense response to the cucumber green mottle mosaic virus infection. *Life*, **11**, 1064.
Souza P.F.N., Garcia-Ruiz H., Carvalho F.E.L. (2019) What proteomics can reveal about plant–virus interactions? Photosynthesis-related proteins on the spotlight. *Theoretical and Experimental Plant Physiology*, **31**, 227–248.
Spanò R., Bottalico G., Corrado A., Campanale A., Di Franco A., Mascia T. (2018) A protocol for producing virus-free artichoke genetic resources for conservation, breeding, and production. *Agriculture*, **8**, 36.
Spanò R., Fortunato S., Linsalata V., D'Antuono I., Cardinali A., de Pinto M.C., Mascia T. (2023) Comparative analysis of bioactive compounds in two globe artichoke ecotypes sanitized and non-sanitized from viral infections. *Plants*, **12**, 1600.
Tanner F., Tonn S., de Wit J., Van den Ackerveken G., Berger B., Plett D. (2022) Sensor-based phenotyping of above-ground plant–pathogen interactions. *Plant Methods*, **18**, 35.
Thorvaldsdóttir H., Robinson J.T., Mesirov J.P. (2013) Integrative genomics viewer (IGV), high performance genomics data visualization and exploration. *Briefings in Bioinformatics*, **14**, 178–192.
Venturini M.T., Araújo T.D., Abreu E.F.M., Andrade E.C.D., Santos V.D., Silva M.R.D., Oliveira E.J.D. (2016) Crop losses in Brazilian cassava varieties induced by the *Cassava common* mosaic virus. *Scientia Agricola*, **73**, 520–524.
Yang Y., Benning C. (2018) Functions of triacylglycerols during plant development and stress. *Current Opinion in Biotechnology*, **49**, 191–198.
Zanini A., Collavino A., Medina R., Celli M., Conci V., Di Feo L. (2020) Influencia de *Cassava common mosaic virus* (CsCMV) en la producción de raíces de plantas de *Manihot esculenta*. *Revista Investigación, Ciencia y Universidad*, **3**, 99.
Zanini A.A., Di Feo L., Luna D.F., Paccioretti P., Collavino A., Rodriguez M.S. (2021) *Cassava common mosaic virus* infection causes alterations in chloroplast ultrastructure, function, and carbohydrate metabolism of cassava plants. *Plant Pathology*, **70**, 195–205.
Zeier J. (2013) New insights into the regulation of plant immunity by amino acid metabolic pathways. *Plant, Cell & Environment*, **36**, 2085–2103.

Plant Biology © 2024 The Author(s). *Plant Biology* published by John Wiley & Sons Ltd on behalf of German Society for Plant Sciences, Royal Botanical Society of the Netherlands.

14388677, 0, Downloaded from https://onlinelibrary.wiley.com/doi/10.1111/plb.13675 by CNR Group, Wiley Online Library on [11/07/2024]. See the Terms and Conditions (https://onlinelibrary.wiley.com/terms-and-conditions) on Wiley Online Library for rules of use; OA articles are governed by the applicable Creative Commons License